

Electronic Supplementary Information

In Situ 2D-Extraction of DNA Wheels by 3D Through-Solution Transport

Yusuke Yonamine*^{a,b}, Keitel Cervantes-Salguero*^c, Waka Nakanishi*^a, Ibuki Kawamata^c,
Kosuke Minami^a, Hirokazu Komatsu^a, Satoshi Murata*^c, Jonathan P. Hill^{a,b}, and Katsuhiko
Ariga*^{a,b}

^a*World Premier International (WPI) Research Centre for Materials Nanoarchitectonics (MANA), National Institute for Materials Science (NIMS) 1-1 Namiki, Tsukuba, Ibaraki, 305-0044, Japan*

^b*CREST, JST, Sanbancho, Chiyoda-ku, Tokyo, 102-0075, Japan*

^c*Department of Bioengineering and Robotics, Tohoku University, 6-6-1 Aobayama, Sendai 980-8579, Japan*

Contents

1. Preparation of the DNA wheel	S2
2. UV-vis absorption and circular dichroism (CD) spectroscopic analysis	S3
3. Dynamic light scattering (DLS) analysis	S3
4. AFM image of DNA wheel-cationic lipid complex cast on mica substrate from chloroform solution	S5
5. AFM images of bare DNA wheel and the complex with cationic lipid on mica	S6
6. Hydrophobic patterning of SiO ₂ wafer	S7
7. AFM images of bare DNA wheels on hydrophilic or hydrophobic substrate	S8
8. AFM images and analysis of DNA wheels on hydrophobic/hydrophilic patterned SiO ₂ wafer surface before and after complexation with cationic lipid	S9

1. Preparation of the DNA wheel

The DNA wheel was assembled by a previously method reported¹ and the size was confirmed. A pair of single-strand DNAs (the motif of DNA wheel; DNA wheel (+) and (-)) were dissolved (1 μ M) in Tris-acetate-EDTA containing magnesium ion buffer (Tris 40 mM, acetate 20 mM, EDTA 1 mM and magnesium acetate 12.5 mM; TAE/Mg²⁺) and annealed at 90 °C. The temperature of the solution was then slowly lowered to 25 °C. Oligomerization was confirmed by native polyacrylamide gel electrophoresis (PAGE) analysis. As a result, the band around 180 bp compared to the single strand of DNA motif (52 base) was observed indicating that most of the DNA motif had formed the wheel structure in solution (Figure S1, green arrow). The size was estimated to be significantly lower than the anticipated value probably due to the highly compact wheel structure.

The sequences (5' to 3') of the DNA motif:

DNA wheel (+):

TCCACGGTCTGCTACTCGGTAATGGCTCATCAAGCGTCCAGTTCCGCAAACG

DNA wheel (-):

CGCTTCGTTTGC GGAACTGGAGATGAGCCATTACCGAGTAGGTGGACAGACC

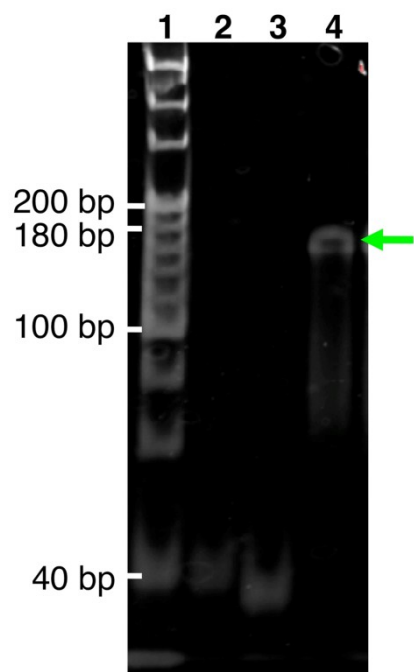


Figure S1. Native polyacrylamide gel electrophoresis (PAGE) of DNA wheel. Lane 1: DNA molecular weight marker. Lane 2: a single strand (+) of DNA wheel motif (52 base). Lane 3: a single strand (-) of DNA wheel motif (52 base). Lane 4: Annealed DNA wheel motif (+) and (-). TBE buffer (89 mM Tris-borate, 2 mM EDTA) was used for migration. The gel was 8% acryl amide and stained with SYBR® Gold nucleic acid gel stain for 10 min.

¹ Hamada, S.; Murata, S. *Angew. Chem. Int. Ed. Engl.* **2009**, *48*, 6820.

2. UV-vis absorption and circular dichroism (CD) spectroscopic analysis

Aqueous solution of dioctadecyldimethylammonium bromide $2C_{18}N^+$ (50 μ L, 2.1 mM; 2 mol equivalents to the phosphate groups of the DNA) was added at room temperature to DNA wheel solution (500 μ L, 1 μ M) in TAE/ Mg^{2+} buffer, and a water-insoluble white precipitate was immediately formed. The product was extracted into chloroform (500 μ L). The absorbance of the organic layer at 260 nm was measured (UV-3600, SHIMADZU) as 0.887 (Figure S2b, red line) while the absorbance of the aqueous layer was significantly decreased to 0.046 (Figure S2b, blue line) compared to the value before extraction (0.932; Figure S2b, black line). The extraction yield was calculated by assuming that the DNA molar extinction coefficient was constant. The lipid-modified DNA wheel in chloroform solution was analyzed by circular dichroism spectroscopy (J-820, JASCO). The spectrum showed a Cotton effect pattern closer to the B-type (Figure S2c, red line). Compared to the standard DNA wheel in TAE/ Mg^{2+} buffer (Figure S2c, black line), the θ value of the positive Cotton effect at 260 nm was slightly increased. This trend is observed in the spectrum of the A-type structure (a DNA structure in dried state), and suggests that the lipid modified DNA is slight dehydrated in an organic solvent. Experimental conditions for the shorter cationic lipid, $2C_{12}N^+$ were same as those of $2C_{18}N^+$. The extraction efficiency was significantly lower than that of $2C_{18}N^+$ due to the lower of hydrophobicity (Fig S2b).

3. Dynamic light scattering (DLS) analysis

The hydrodynamic sizes of bare (10 μ M in TAE/ Mg^{2+} buffer) and lipid-modified DNA wheel (10 μ M in chloroform) and vesicles of $2C_{18}N^+$ (10 mM in H_2O) were analyzed by DLS measurement (DelsaNano C, Beckman-Coulter) as intensity distributions. In the case of bare DNA wheels, the size distribution was 31 ± 9 nm (Figure 2a, blue). Although the theoretical diameter of the DNA wheel is about 40 nm, the shape is disk-like with a thickness of 1.5 nm, so that the hydrodynamic radius ought to be correspondingly smaller. In the case of the lipid-modified DNA sample, the peaks of 45 ± 9 nm and larger size (>2000 nm) were observed (Figure 2a, green). These peaks were clearly different from the peak of lipids alone forming a vesicle structure (174 ± 82 nm). The former was attributed to the lipid-modified DNA wheel. The latter large structure may be due to irreversible aggregation. At the lipid modification step in an aqueous solution, lipid-modified DNA was collected as a water insoluble precipitate and can form aggregates that are not relaxed even in organic solvents.

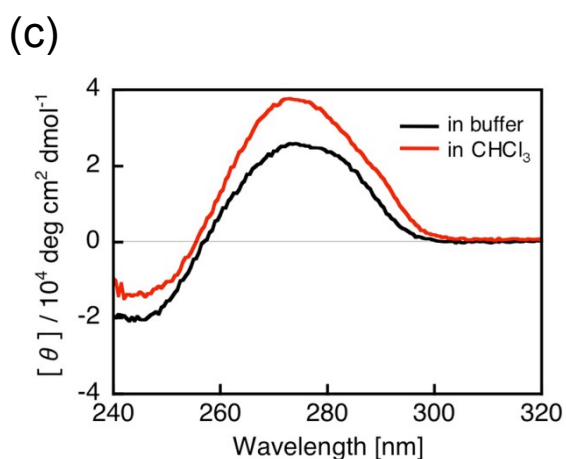
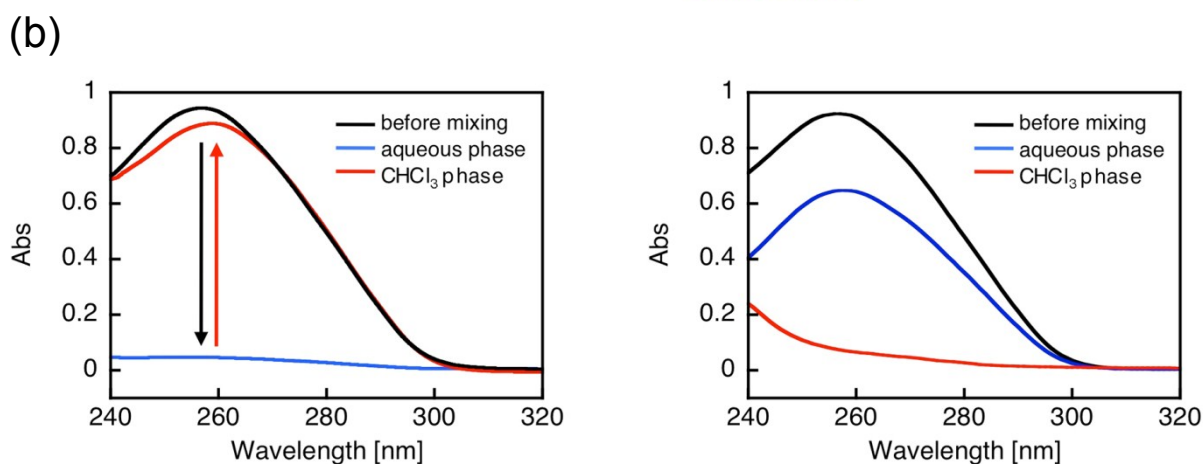
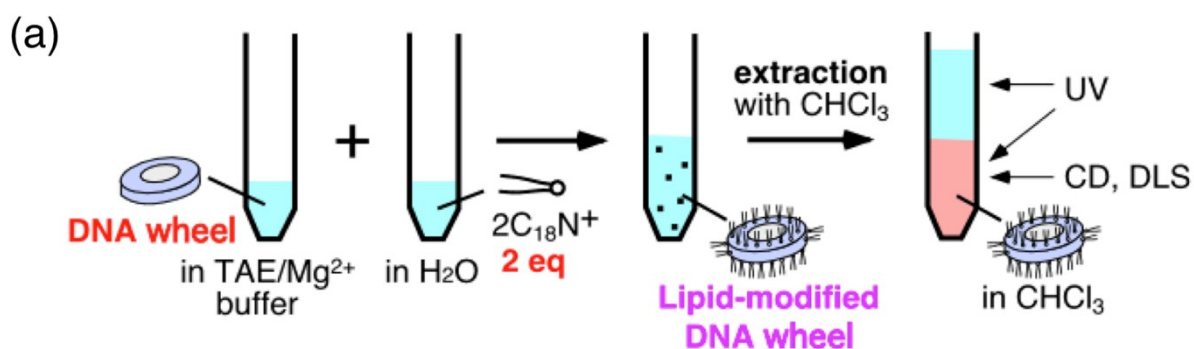


Figure S2. Preparation and characterization of lipid-modified DNA wheel in solution. (a) Schematic diagrams of formation in aqueous phase and extraction into organic phase of lipid-modified DNA wheel. (b) UV-Vis spectra of organic phase (red line) and water phase before (black line) and after (blue line) extraction. Baseline: CHCl₃ (red line) and TAE/Mg buffer (black and blue lines), respectively. Left: 2C₁₈N⁺; Right: 2C₁₂N⁺ (c) CD spectra of organic phase (red line) and water phase before (black line) for 2C₁₈N⁺. Baseline: CHCl₃ (red line) and TAE/Mg buffer (black and blue lines), respectively.

4. AFM image of DNA wheel-cationic lipid complex cast on mica substrate from chloroform solution

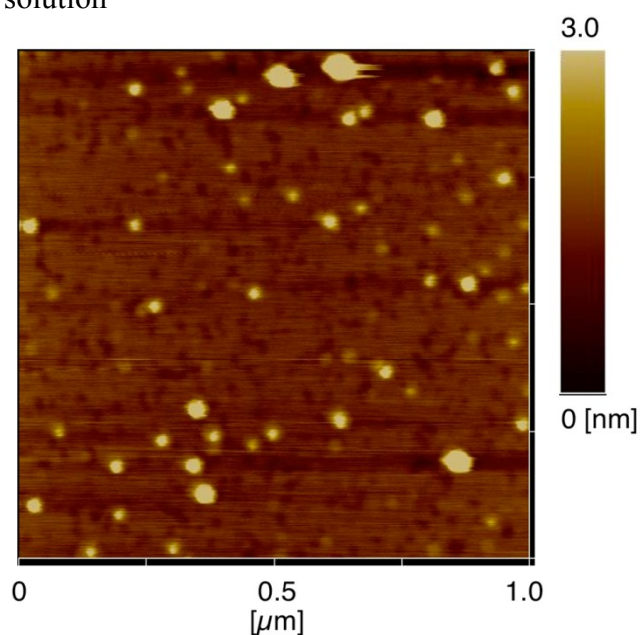


Figure S3. AFM image of DNA wheel-cationic lipid complex casted on mica substrate from chloroform solution. The image was taken under dry conditions. AFM imaging was performed using an AFM system (Nanoscope V, Bruker) with a cantilever operating in dynamic force mode (SI-DF20, Hitachi High-Tech Science). The chloroform solution was prepared by the same method as described in 2. UV-vis absorption and circular dichroism (CD) spectroscopic analysis. Frame rate: 260 [sec/frame]

5. AFM images of bare DNA wheel and the complex with cationic lipid on mica.

DNA wheel solution (1 μM) in TAE/ Mg^{2+} buffer was deposited on a freshly cleaved mica substrate for 5 min, and the substrate was rinsed with TAE/ Mg^{2+} buffer three times. AFM imaging was performed using a high-speed AFM system (Nano Live Vision, RIBM) with a silicon nitride cantilever (BLAC10EGS-A2, Olympus) in solution phase using TAE/ Mg^{2+} buffer as observation solution (Figure S4). For this system, TAE/ Mg^{2+} buffer was replaced with lipid solution (didodecyldimethylammonium bromide; $2\text{C}_{12}\text{N}^+$: $9\mu\text{g}/\text{mL}$ in TAE/ Mg^{2+}) as observation buffer, and the lipid modification process was monitored. Since cationic lipid with longer alkyl chain ($2\text{C}_{18}\text{N}^+$) needs pre-heating before use to dissolve in buffer, shorter $2\text{C}_{12}\text{N}^+$ was used instead. For observation of DNA wheels by images were obtained at the frame rate of 50 sec/frame unless otherwise mentioned.

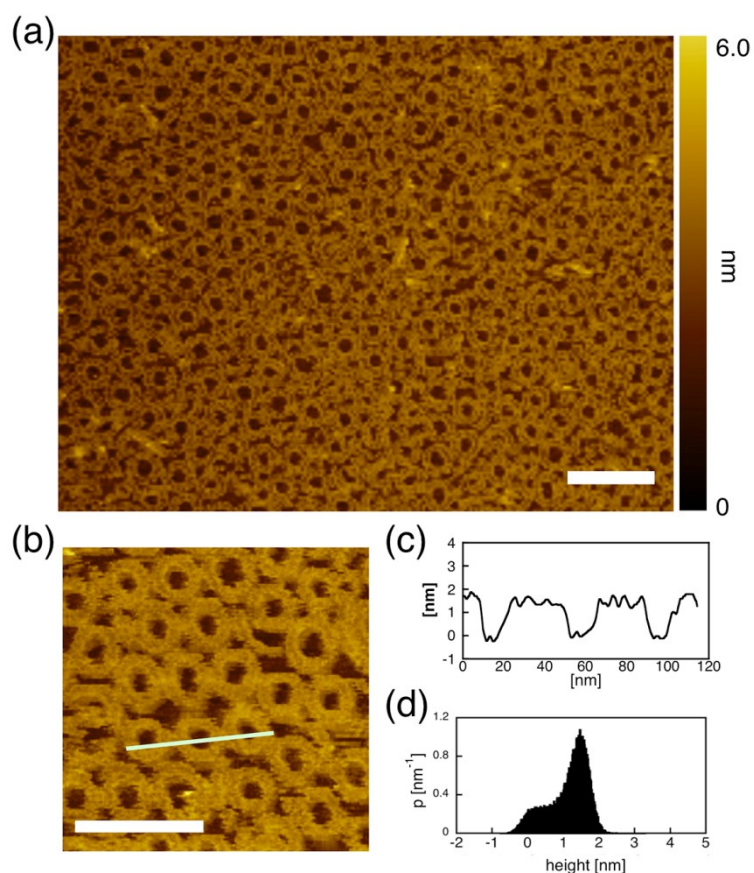


Figure S4. (a, b) AFM images of DNA wheel on mica surface. Observation solution: TAE/ Mg^{2+} buffer. (c, d) Height profile (c) and distributions (d) of the image (b). Scale bars: 100 nm. Density of the height distribution (ρ) was calculated by statistical functional tool of Gwyddion software,² and the lower peak top of the bimodal distribution was assumed to be the height of the mica surface.

² Nečas, D.; Klapetek, P. *Cent. Eur. J. Phys.* **2012**, *10*, 181.

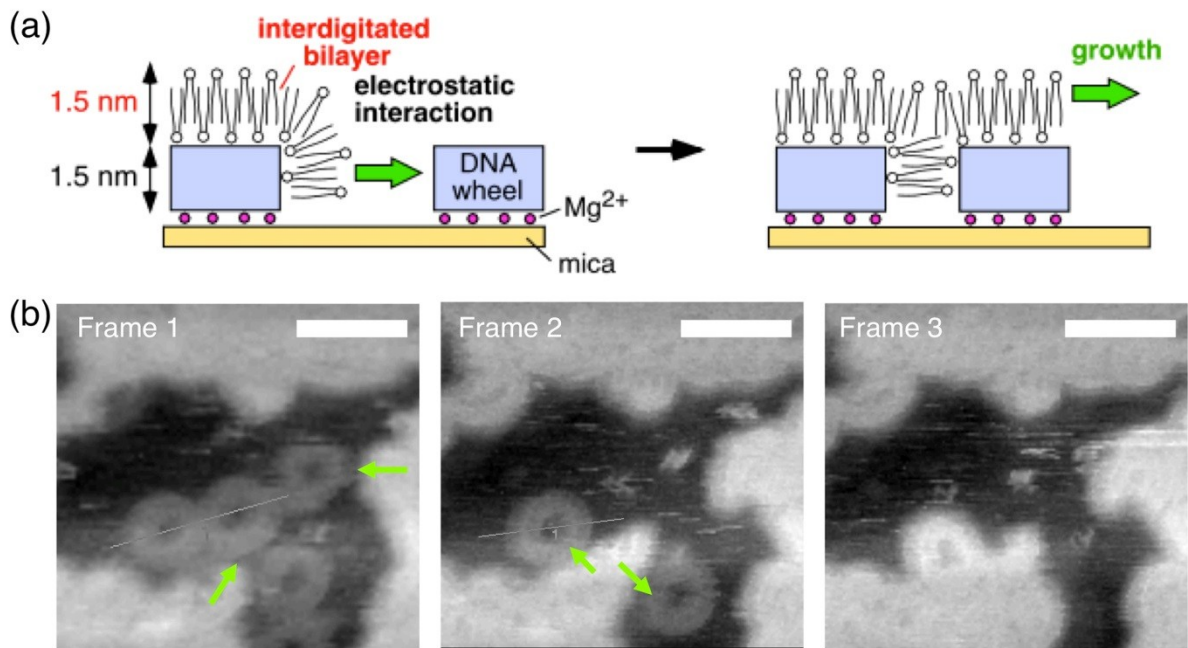


Figure S5. Lipid modification process. (a) Schematic diagrams of a conceivable mechanism. Electrostatic interaction between anionic phosphate of DNA and cationic lipid. Formation of interdigitated bilayer is expected from the height. (b) Sequential AFM images of DNA wheel incorporation process with lipid bilayer growth. The image was taken every 1 min. Scale bars: 50 nm.

6. Hydrophobic patterning of SiO₂ wafer

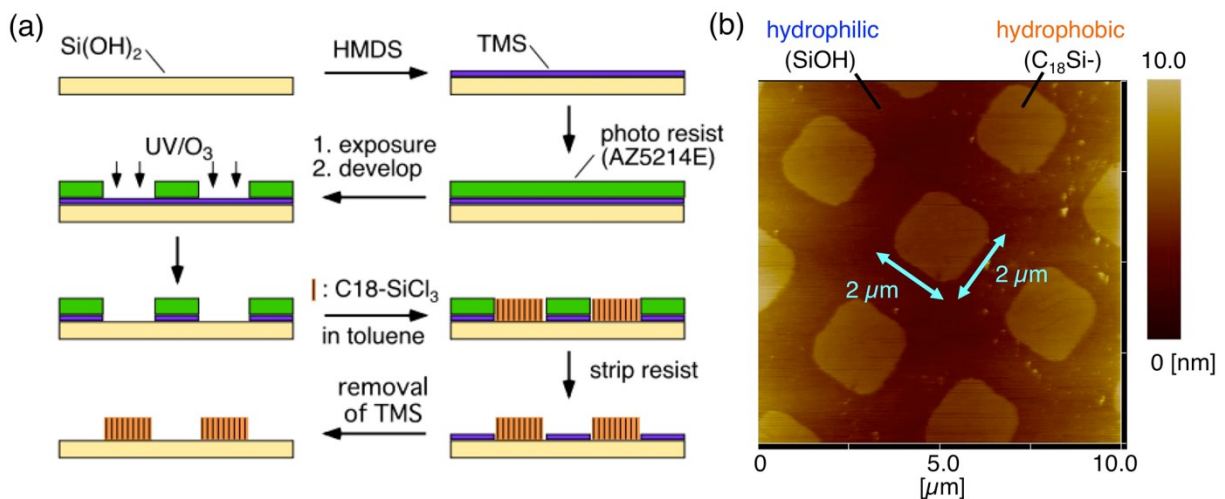


Figure S6. (a) A schematic diagram of alkyldisilane (C₁₈) patterning on SiO₂ wafer. (b) AFM image of the C₁₈ patterned SiO₂ wafer surface in air phase. AFM imaging was performed using AFM system (Nanoscope V, Bruker) with a cantilever for a dynamic force mode (SI-DF40, Hitachi High-Tech Science). Frame rate: 260 [sec/frame]

7. AFM images of bare DNA wheels on hydrophilic or hydrophobic substrate

SiO₂ wafer and C₁₈ patterned SiO₂ wafer were treated with piranha solution (H₂O₂ (30%): H₂SO₄ (96%) = 1:2) for 30 seconds and rinsed with pure water three times before use. The DNA wheel solution (0.1 μM) in Tris-acetate-EDTA containing magnesium ion buffer (Tris 40 mM, acetate 20 mM, EDTA 1 mM and magnesium acetate 125 mM; TAE/10Mg²⁺) was deposited on the washed surfaces (SiO₂, C₁₈ coated SiO₂ and C₁₈ patterned SiO₂ wafers) for 10 min, and the substrate was rinsed with TAE/10Mg²⁺ buffer three times. AFM imaging was performed using a high-speed AFM system (Nano Live Vision, RIBM) with a silicon nitride cantilever (BLAC10EGS-A2, Olympus) in solution phase using TAE/10Mg²⁺ buffer as observation solution (Figure 3a and S7). For this system, lipid solution (didodecyldimethylammonium bromide; 2C₁₂N⁺: 9 μg/mL in TAE/Mg²⁺) was replaced as the observation solution, and the lipid modification process was monitored (Figure 3b).

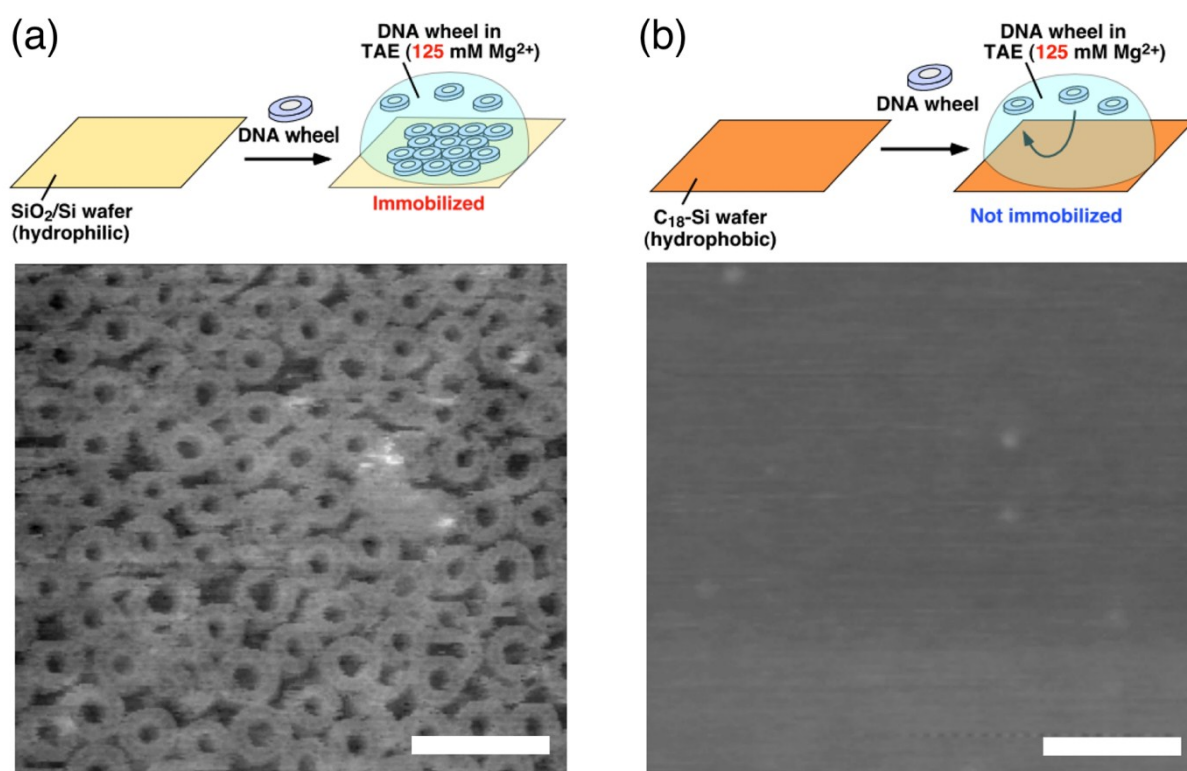


Figure S7. AFM images of adsorption of bare DNA wheel on SiOH (a) or octadecylsilyl coated (b) surface. Scale bars: 100 nm.

8. AFM images and analysis of DNA wheels on hydrophobic/hydrophilic patterned SiO₂ wafer surface before and after complexation with cationic lipid

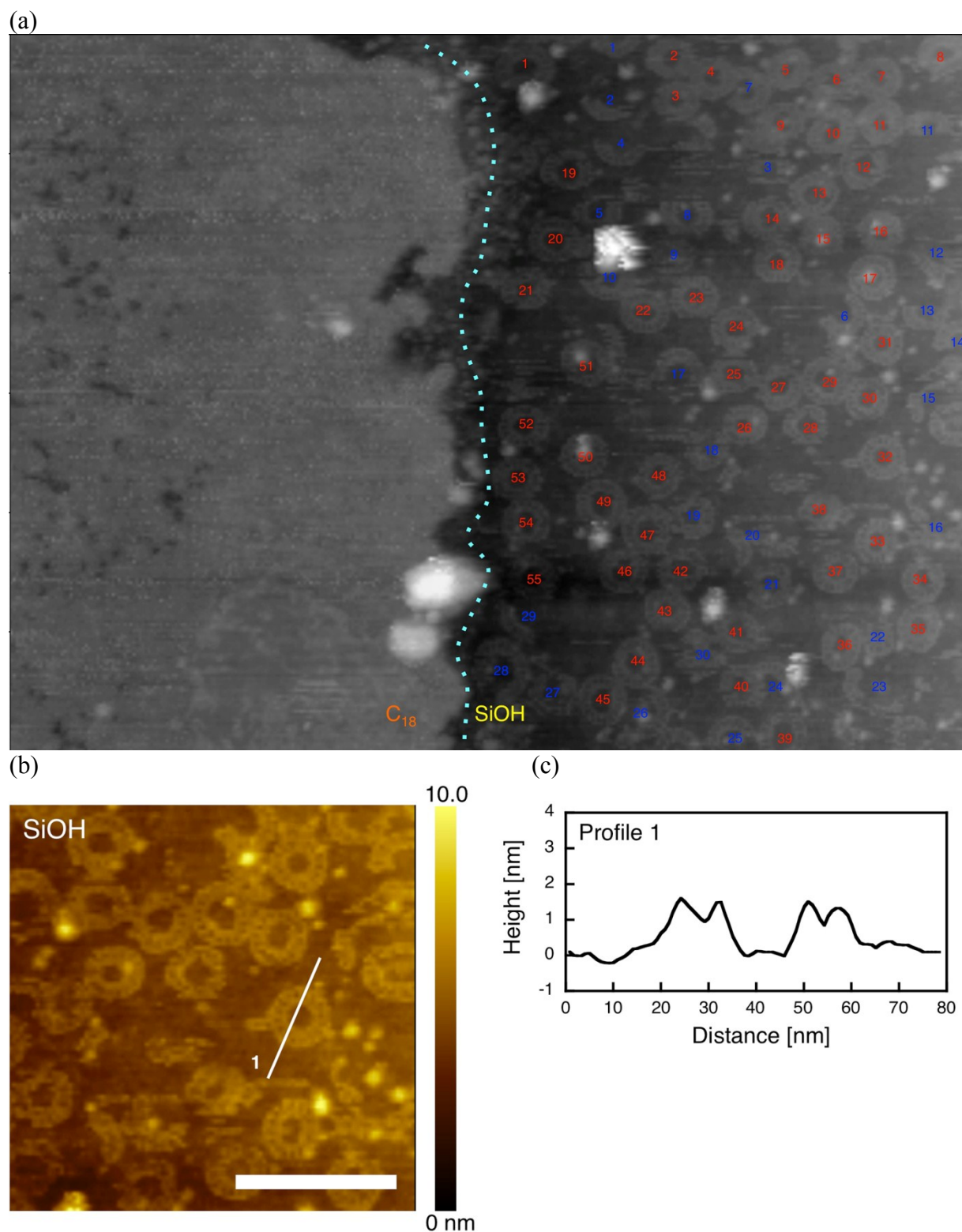


Figure S8. DNA wheels on C₁₈ patterned SiO₂ wafer before lipid-modification. (a) The numbers of the closed (red) and opened (blue) wheels on the SiOH region are 55 and 30, respectively. The size of the image is 800 nm x 600 nm. (b) Magnification of the wheels on hydrophilic surface. Scale bar: 100 nm. (c) Height profile of the lined position in b.

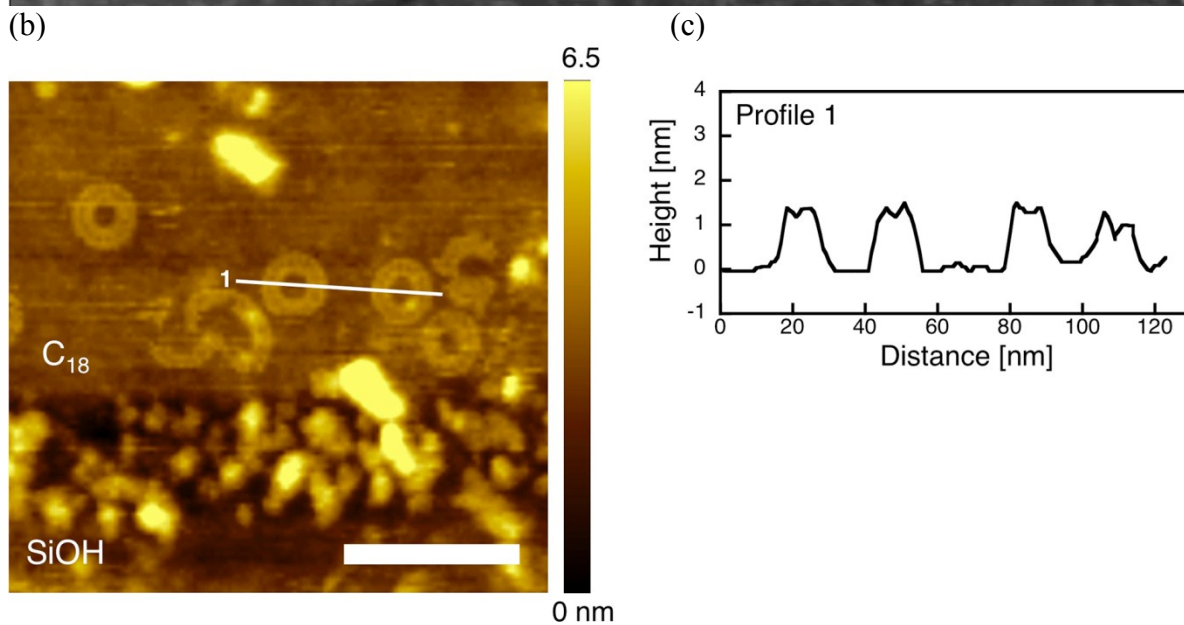
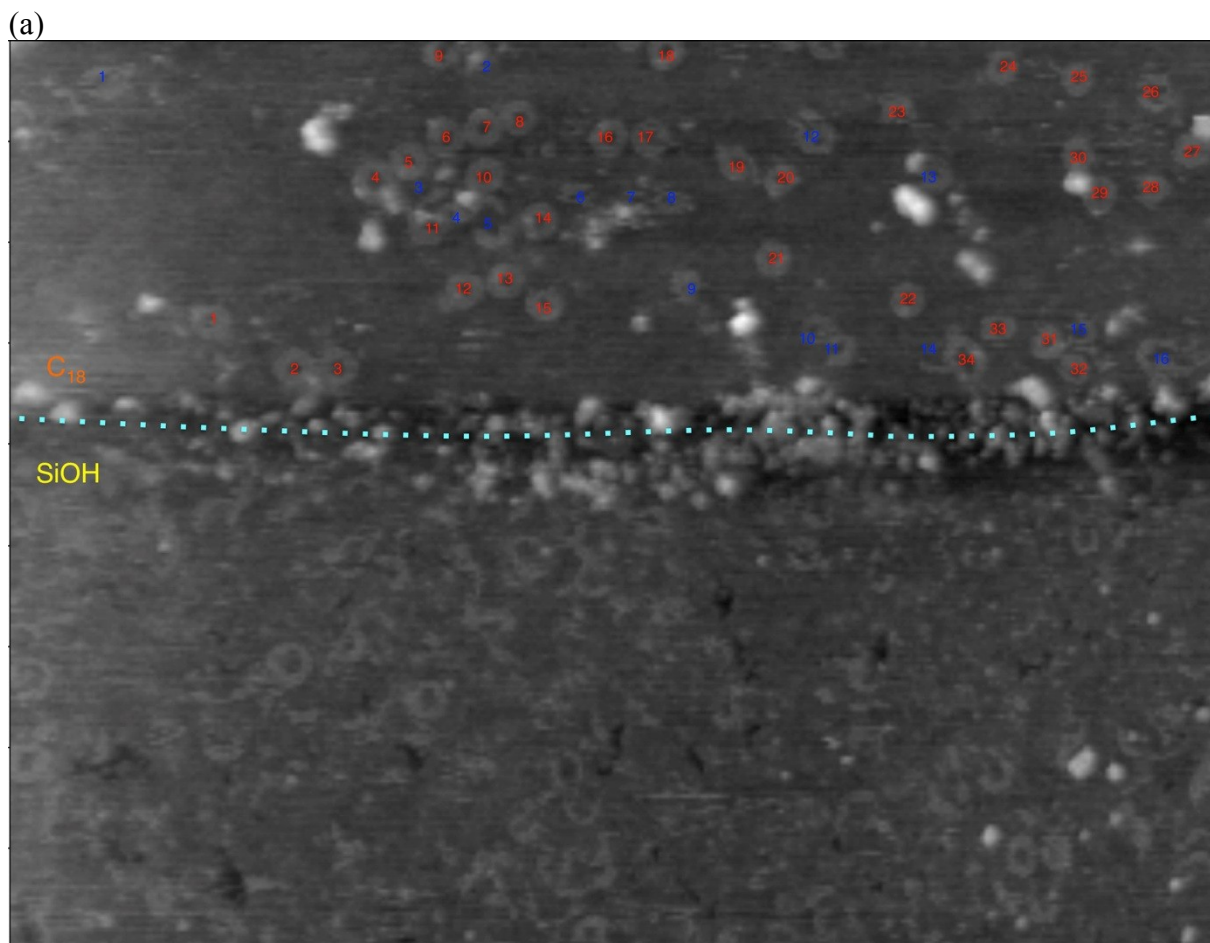
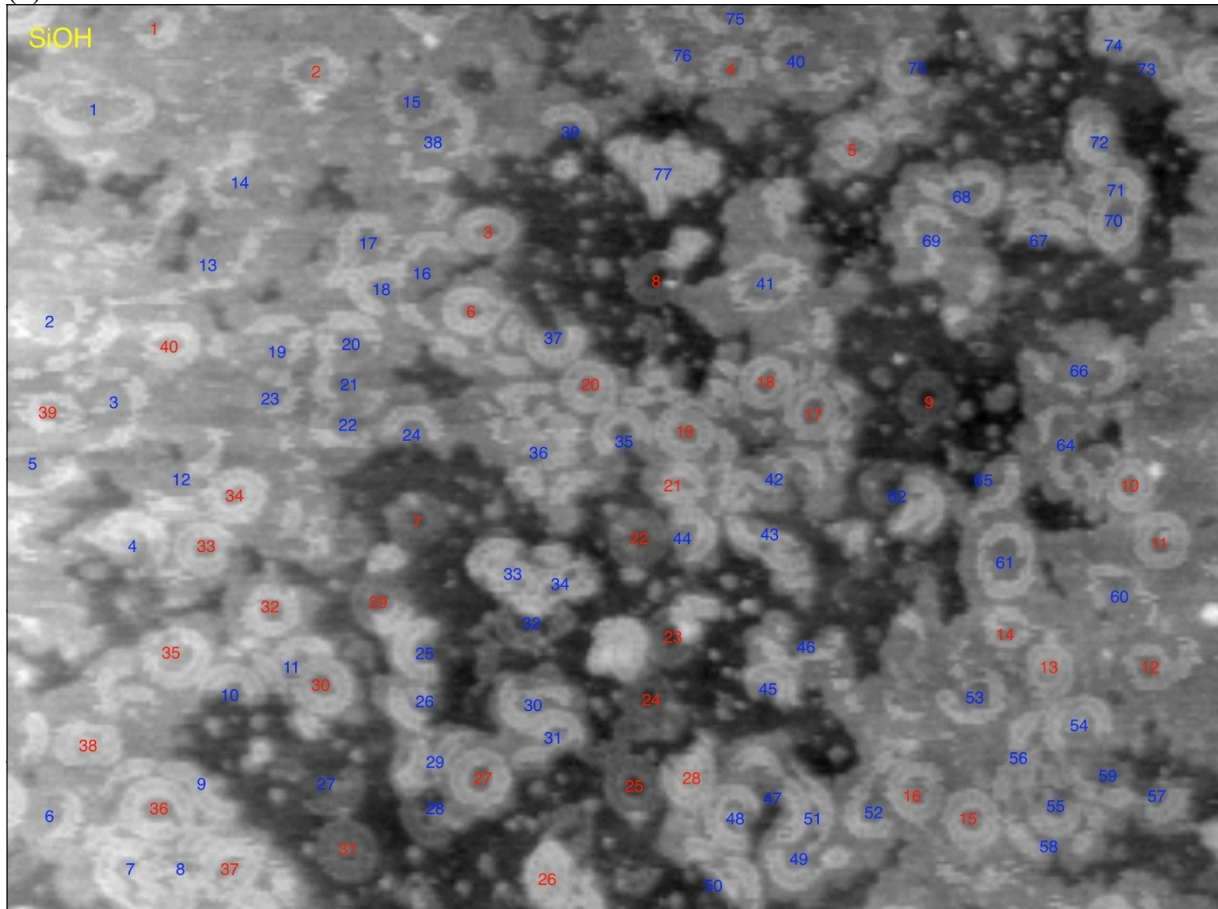
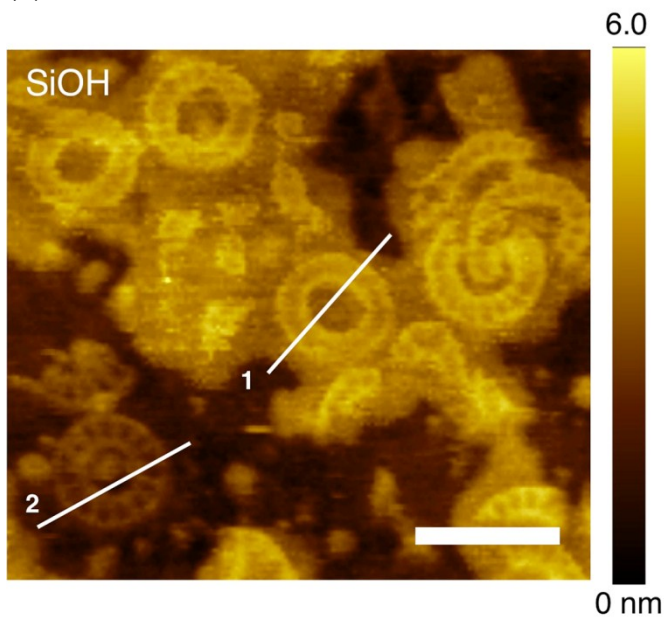


Figure S9. DNA wheels on C_{18} patterned SiO_2 wafer after lipid-modification. The numbers of the closed (red) and opened (blue) wheels on the C_{18} region are 34 and 16, respectively. The size of the image is 1200 nm x 900 nm. The image was taken 22 min after adding the cationic lipid ($2C_{12}N^+$). (b) Magnification of the wheels near the hydrophobic/hydrophilic boundary. Scale bar: 100 nm. (c) Height profile of the lined position in b.

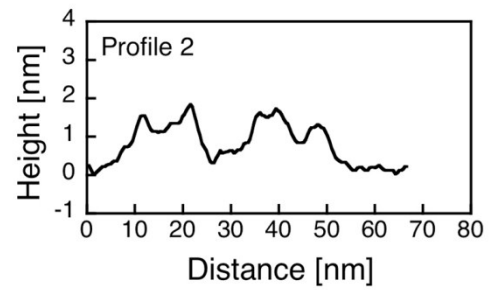
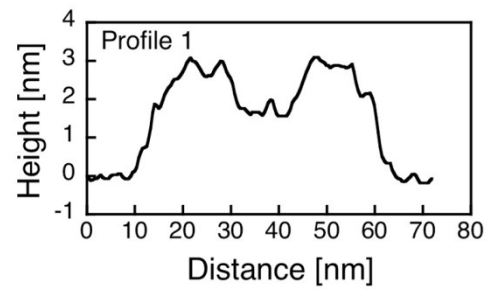
(a)



(b)



(c)



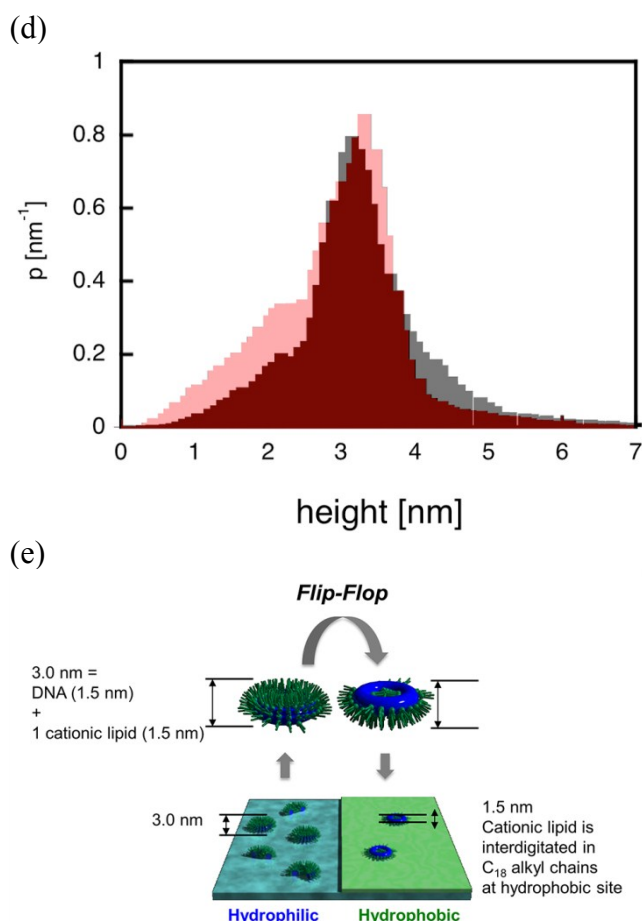


Figure S10. DNA wheels on C₁₈ patterned SiO₂ wafer after lipid-modification (magnified SiOH region). The numbers of the closed (red) and opened (blue) wheels on the SiOH region are 40 and 77, respectively. The size of the image is 800 nm x 600 nm. The image was taken 33 min after adding the cationic lipid (2C₁₂N⁺). (b) The magnification of the wheels on hydrophilic surface. Scale bars: 100 nm (b) Height profile of the lined position in b. (b) Magnification of the wheels on hydrophilic surface. Scale bar: 100 nm. (c) Height profiles of the lined positions in b. (d) Height distribution of DNA-wheel immobilized surface before (red) and after (gray, Fig. 3d, 17 min) the addition of lipid 2C₁₂N⁺. Peak tops of two histograms have essentially the same values (3.2 nm). The data suggests further cationic lipids were not attached on the C₁₈ areas after the addition of 2C₁₂N⁺. (e) Schematic view of DNA wheels and their height after addition of the cationic lipid.

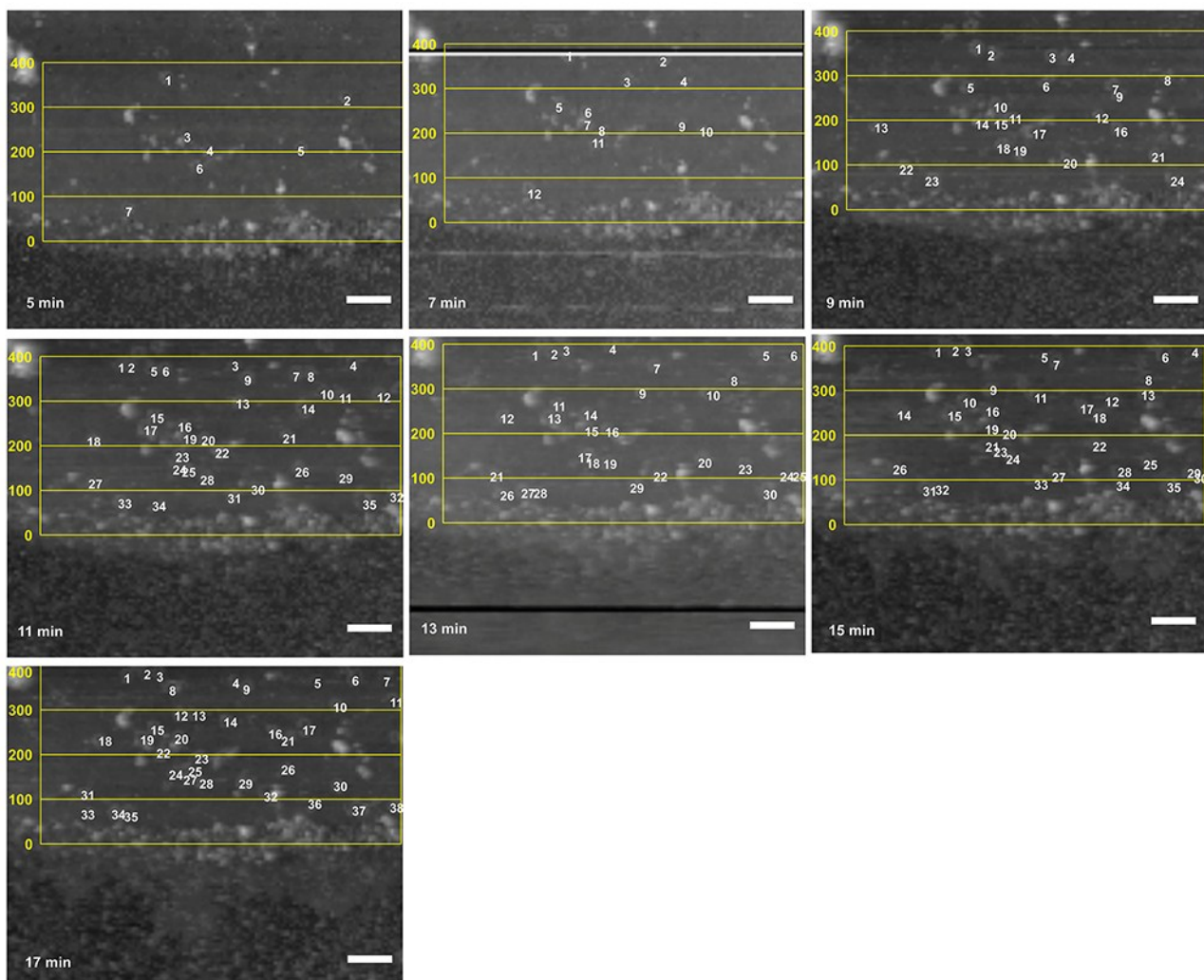


Figure S11. Sequential AFM images of DNA wheel migration to the hydrophobic region from 5 min to 17 min after addition of the cationic lipid ($2C_{12}N^+$). Lines indicate the distance from the hydrophilic/hydrophobic boundary. Sum of opened and closed wheels were counted and are indicated. Only opened wheels with over 50% of the structure remaining were counted. Scale bars: 100 nm.

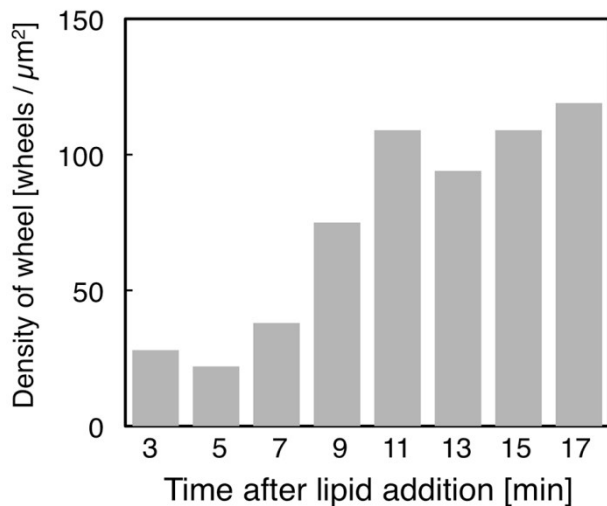


Figure S12. Time course of averaged density of DNA wheel-cationic lipid complex on hydrophobic site (0-400 nm from the hydrophilic/hydrophobic boundary) after complexation with cationic lipid ($2\text{C}_{12}\text{N}^+$).

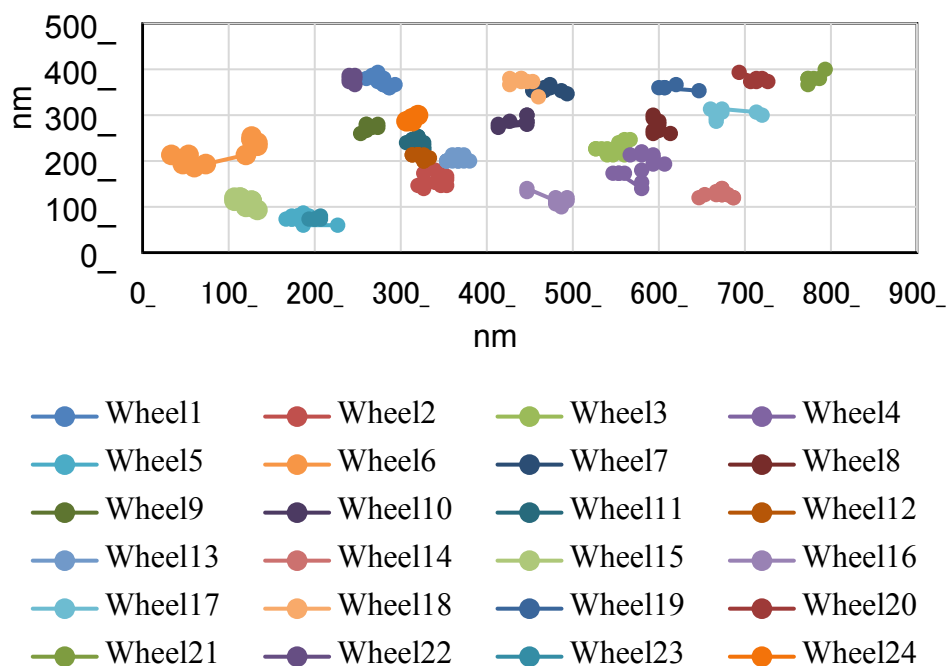


Figure S13. Time-dependent position of wheels. Time after addition of the cationic lipid $2\text{C}_{12}\text{N}^+$: 3 min to 17 min, every 1 min.

Table S1. Estimated diffusion coefficient (D) from the trajectories of wheels by mean-square displacement (MSD).³ The linear dependence of MSD on time t indicates random Brownian diffusion D [$\text{MSD}(t)=4Dt$].

	D [nm^2/sec]
Wheel 1	0.31
Wheel 2	0.31
Wheel 3	0.31
Wheel 4	0.99
Wheel 5	1.17
Wheel 6	4.53
Wheel 7	0.65
Wheel 8	0.57
Wheel 9	0.16
Wheel 10	0.41
Wheel 11	0.20
Wheel 12	0.11
Wheel 13	0.14
Wheel 14	0.18
Wheel 15	0.17
Wheel 16	0.44
Wheel 17	2.06
Wheel 18	1.26
Wheel 19	0.74
Wheel 20	0.71
Wheel 21	0.87
Wheel 22	0.24
Wheel 23	0.14
Wheel 24	0.13
Average: 0.7 ± 0.9 [nm^2/sec]	

³ Anthony, S.; Zhang, L.; Granick, S. *Langmuir* **2006**, *22*, 5266.